

Mimicking Chitin: Chemical Synthesis, Conformational Analysis, and Molecular Recognition of the $\beta(1\rightarrow3)$ *N*-Acetylchitopentaose Analogue

Maria Morando,^[a] Yanping Yao,^[b, c] Sonsoles Martín-Santamaría,^[d] Zhenyuan Zhu,^[b, c] Tong Xu,^[c] F. Javier Cañada,^[a] Yongmin Zhang,^{*, [b, c]} and Jesús Jiménez-Barbero^{*, [a]}

Abstract: Mimicking Nature by using synthetic molecules that resemble natural products may open avenues to key knowledge that is difficult to access by using substances from natural sources. In this context, a novel *N*-acetylchitooligosaccharide analogue, β -1,3-*N*-acetamido-gluco-pentasaccharide, has been designed and synthesized by using aminoglucose as the starting material. A phthalic group has been employed as the protecting group of the amine moiety, whereas a thioalkyl was used as

the leaving group on the reducing end. The conformational properties of this new molecule have been explored and compared to those of its chito analogue, with the β -1,3 linkages, by a combined NMR spectroscopic/molecular modeling approach. Furthermore,

Keywords: conformation analysis • glycomimetics • molecular recognition • NMR spectroscopy • synthetic methods

the study of its molecular recognition properties towards two proteins, a lectin (wheat germ agglutinin) and one enzyme (a chitinase) have also been performed by using NMR spectroscopy and docking protocols. There are subtle differences in the conformational behavior of the mimetic versus the natural chitooligosaccharide, whereas this mimetic is still recognized by these two proteins and can act as a moderate inhibitor of chitin hydrolysis.

Introduction

N-Acetylchitooligosaccharides are involved in a variety of biological events. Apart from being part of the exoskeleton of different insects and fungi, they can also act as chemical signals in plant-induced resistance and are essential parts of the lipopolysaccharides, which behave as nodulation factors.^[1] The use of mimetics (in this case, glycomimetics) is of paramount importance to further evaluate these key processes, from understanding the recognition process, to exploring the mechanisms and finding molecules with enhanced activities. Chitin oligosaccharides (COs, *N*-acetylchitooligosaccharides) and chitosan oligosaccharides (CSOs, chitooligosaccharides) are ubiquitous potential external chemical signals,^[1,2] derived by many chitinases from the cell walls of fungi or the degradation of insoluble chitin.

[a] M. Morando,[†] F. J. Cañada, J. Jiménez-Barbero
Chemical and Physical Biology, Centro de Investigaciones Biológicas, CSIC, Ramiro de Maeztu 9
28040 Madrid (Spain)
Fax: (+34)915360432
E-mail: jjbarbero@cib.csic.es

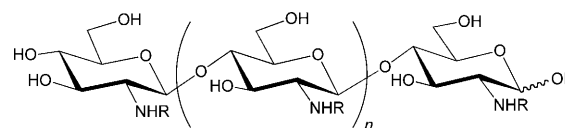
[b] Y. Yao,[†] Z. Zhu, Y. Zhang
Université Pierre & Marie Curie-Paris 6
Institut Parisien de Chimie Moléculaire (UMR 7201)
C 181, 4 place Jussieu, 75005 Paris (France)
Fax: (+33)1-4427-5504
E-mail: yongmin.zhang@upmc.fr

[c] Y. Yao,[†] Z. Zhu, T. Xu, Y. Zhang
Institute of Biotechnology, College of Agriculture Biotechnology
Zhejiang University, Hangzhou 310029 (China)

[d] S. Martín-Santamaría
Department of Chemistry, Faculty of Pharmacy
Universidad San Pablo CEU, Boadilla del Monte
28668 Madrid (Spain)

[†] These two authors have equally contributed to this work.

Supporting information for this article is available on the WWW under <http://dx.doi.org/10.1002/chem.200902860>. It contains all the details of the calculations for the molecular modeling, the Φ and Ψ variations of every β GlcNAc1-3GlcNAc glycosidic linkage during the vacuum (two force fields), solvated MD simulations, and sections of NMR spectra.



chitin oligosaccharides: R=Ac
chitosan oligosaccharides: R=H

N-Acetylchitooligosaccharides and chitooligosaccharides, composed of 2-deoxy-2-acetamido-*D*-glucopyranosyl residues and 2-deoxy-2-amido-*D*-glucopyranosyl residues, respectively, are important structural parts of glycans, glycopeptides, and glycoproteins. Chitin oligosaccharides and their derivatives play an important role as signal molecules in plant and animal processes, and they are involved in developmental and defense-related signaling pathways.^[3] After binding with members of the GhCTL group (a new group of chitinase-like proteins), chitin oligosaccharides are also essential for cellulose synthesis in primary and secondary cell walls.^[4]

Although the defense mechanism against pathogens has become increasingly apparent, little is known about the mechanisms of the COs molecular signals perceived by cells and about the molecular structures of COs responsible for induced resistance; even very little is known about the molecular basis of the signal transduction pathways underlying oligosaccharide recognition processes. Even more, it is hard to understand the determinant specificity of oligosaccharide recognition processes.^[5]

The induced activity of COs and CSOs is determined by both the molecular weight and the degree of acylation/acylation, and the molecular weight is directly influenced by the degree of polymerization (DP).^[6] Besides, the main backbone of COs, sugar residues, and the different substituents could all influence the plant-induced resistance of COs.

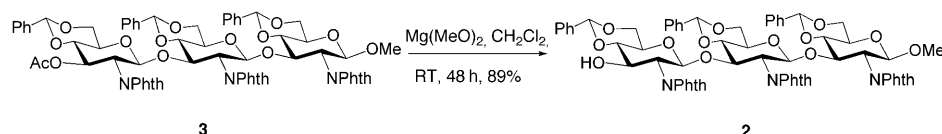
Mimicking nature by using synthetic molecules that resemble natural products may open avenues to key knowledge that is difficult to access by using substances from natural sources. In particular, the oligosaccharides obtained from natural sources are not suitable for studies on the mechanism of induced resistance due to their complicated compositions, varied molecular weight, and the difficulty in isolating a pure component from natural products. Chemical synthesis could be used to obtain pure oligosaccharides with explicit structures, which are appropriate for the induced-resistance study. To know whether the β -1,4 linkage is essential in keeping the biological properties of these molecules, it is important to synthesize a series of chitin oligosaccharide analogues possessing a different backbone linkage (for example, a β -1,3 linkage), to explore the plant-induced resistance elicited by these chitin oligosaccharide derivatives.

In our previous work, we have synthesized two chitin oligosaccharide analogues, β -1,3-*N*-acetyl-glucosamine disaccharide and β -1,3-*N*-acetyl-glucosamine trisaccharide.^[7] Herein, we report the first synthesis of β -1,3-*N*-acetyl-glu-

cosamine pentasaccharide to be used as a tool for initial interaction studies as a ligand or inhibitor for lectins and enzymes involved in the recognition and metabolism of chitooligosaccharides. The knowledge derived from this study would be of importance for further investigation of the function of COs signals in plants and in defense mechanisms.

Results

Synthesis: A key building block in the synthesis of pentasaccharide **1** was methyl (4,6-*O*-benzylidene-2-deoxy-2-phthalimido- β -*D*-glucopyranosyl)-(1 \rightarrow 3)-(4,6-*O*-benzylidene-2-deoxy-2-phthalimido- β -*D*-glucopyranosyl)-(1 \rightarrow 3)-4,6-*O*-benzyl-

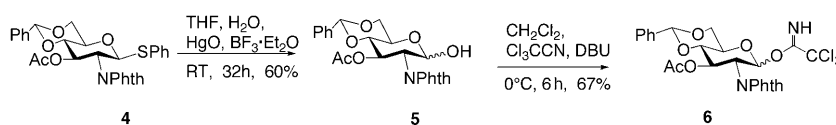


Scheme 1. Synthesis of the trisaccharide acceptor **2**.

idene-2-deoxy-2-phthalimido- β -*D*-glucopyranoside (**2**), which could be readily prepared from the known trisaccharide **3**^[7] by deacetylation with a $Mg(OMe)_2$ solution, as shown in Scheme 1.

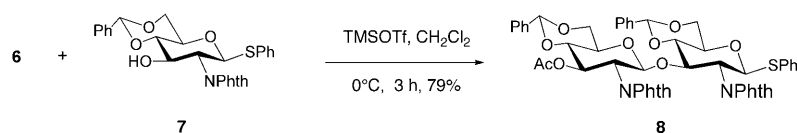
Compound **2** was obtained after stirring for 48 h in dry dichloromethane at room temperature. The trisaccharide **2** has a free hydroxyl group at C-3'', plus a methyl group at C-1, which can then be used as an acceptor in the next glycosylation reaction.

For the synthesis of the pentasaccharide **1**, a 2+3 block-synthesis strategy was used. Treatment of the known compound **4**^[8] with $BF_3 \cdot Et_2O/HgO$ gave a hemiacetal **5**, which was used directly for the next step without further characterization. Reaction of **5** with $Cl_3CCN/1,8$ -diazabicyclo[5.4.0]undec-7-ene (DBU) gave the trichloroacetimidate **6** in 40% yield (for two steps), as shown in Scheme 2. The ¹H NMR spectrum showed that the imidate was formed essentially in the β form ($J_{1,2} = 8.8$ Hz).

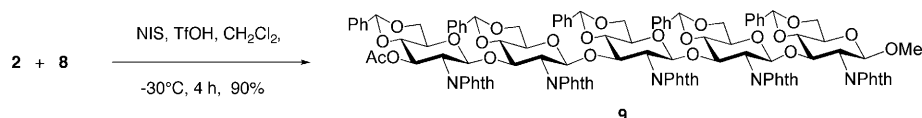


Scheme 2. Synthesis of the donor **6**.

Condensation of **6** with the previously described **7**,^[9] in the presence of trimethylsilyl triflate (TMSOTf) and dichloromethane, gave β (1 \rightarrow 3)-linked disaccharide **8** in 79% yield (Scheme 3). Its stereochemistry was determined to be the desired β form on the basis of the H-1',H-2' coupling constant ($J_{1,2} = 8.0$ Hz).

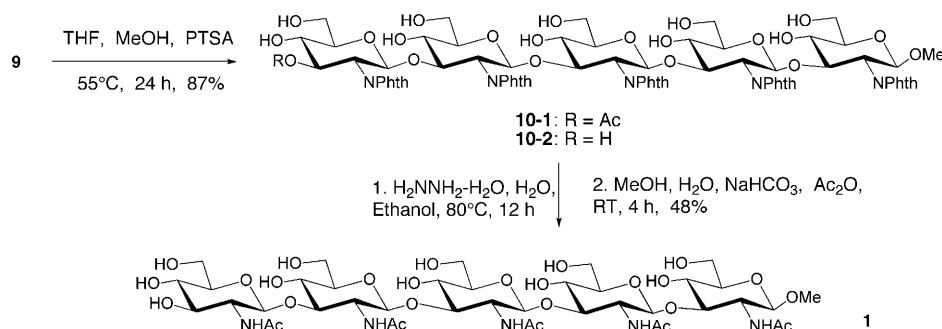
Scheme 3. Synthesis of the disaccharide donor **8**.

The glycosylation of the trisaccharide **2** with donor **8** was achieved in the presence of *N*-iodosuccinimide (NIS)-trifluoromethanesulfonic acid (TfOH) in dry dichloromethane (with 4 Å ground molecular sieves) for 4 h at −30°C, providing the desired pentasaccharide **9** in 90% yield (Scheme 4).

Scheme 4. Synthesis of the protected pentasaccharide **9**.

The stereochemistry of the newly introduced linkage was determined to be β, on the basis of the GlcN H-1,H-2 coupling constant ($J_{1,2}=8.4$ Hz).

Deprotection of the benzylidene groups of **9** was first performed by the classical hydrogenolysis method. Surprisingly, the desired compound could not be isolated from the reaction mixture after testing a variety of reaction times, solvents, and amounts of catalyst. An alternative method was then used. Treatment of pentasaccharide **9** with *p*-toluenesulfonic acid (PTSA) in THF and methanol for 24 h at 55°C gave a mixture of two compounds **10-1** and **10-2** in 87% yield and in a 3:1 ratio (Scheme 5).

Scheme 5. Deprotection and *N*-acetylation of the pentasaccharide.

After separation, the MS analysis revealed that **10-1** is the desired 4,6-*O*-debenzylidene product, whereas **10-2** is a derivative of 3e-deacetylated **10-1**. These two compounds were both used for the next reaction without further characterization. Treatment of **10-1** and **10-2** with hydrazine hydrate and water in boiling ethanol, followed by acetylation with acetic anhydride and NaHCO₃ in water and methanol

was performed. Purification of the product was performed by chromatography on Sephadex G25 (H₂O), to provide the desired β-1→3-*N*-acetyl-glucosamine pentasaccharide (**1**) in 48% yield (for two steps), as shown in Scheme 5.

NMR spectroscopic data and assignment: All the details of the NMR experiments are given in the material and methods sections. The combination of selective 1D-TOCSY, selective 1D-NOESY, 2D-NOESY, 2D-TOCSY (in D₂O and H₂O/D₂O), and 2D-HSQC experiments^[10] permitted assignment of all the resonances of the pentasaccharide **1** (see the Supporting Information). As frequently found in carbohydrates, severe overlap within the ring proton region was found. Fortunately, there was a distinction between the signals arising from the different residues within the amide region, which was evaluated by running experiments in H₂O.

As an example, sections of the TOCSY and HSQC spectra recorded at 800 MHz and 298 K are presented in Figure 1. The behavior of the amide protons with temperature is also given. Second-order effects were found in the anomeric protons even at 800 MHz, as depicted in the Supporting Information. However, the recording of the spectra at different temperatures permitted us to evaluate the couplings and to assign most of the signals. In any case, the analysis of the coupling constants and the NOE patterns allowed us to establish that the pyranoid rings adopt the expected ⁴C₁ chair conformations. The chemical shifts are given in Table 1.

To properly evaluate the NOEs, and to discard the possibility of aggregates at the working concentration, NMR diffusion order spectroscopy (DOSY) experiments^[11] were used to confirm the aggregation state of the molecules for the employed experimental conditions. It was confirmed that, at the working concentration (ca. 1–2 mM), the molecule behaved

as a monomer, since at these concentrations the diffusion coefficient was basically identical to that previously reported for the chitin pentasaccharide.^[11] Thus, the experimental data can be unambiguously correlated with a single species.

After assignment of the key protons, emphasis was placed on the inter-residual NOEs and those connecting the different fragments of the molecules. It was observed that every

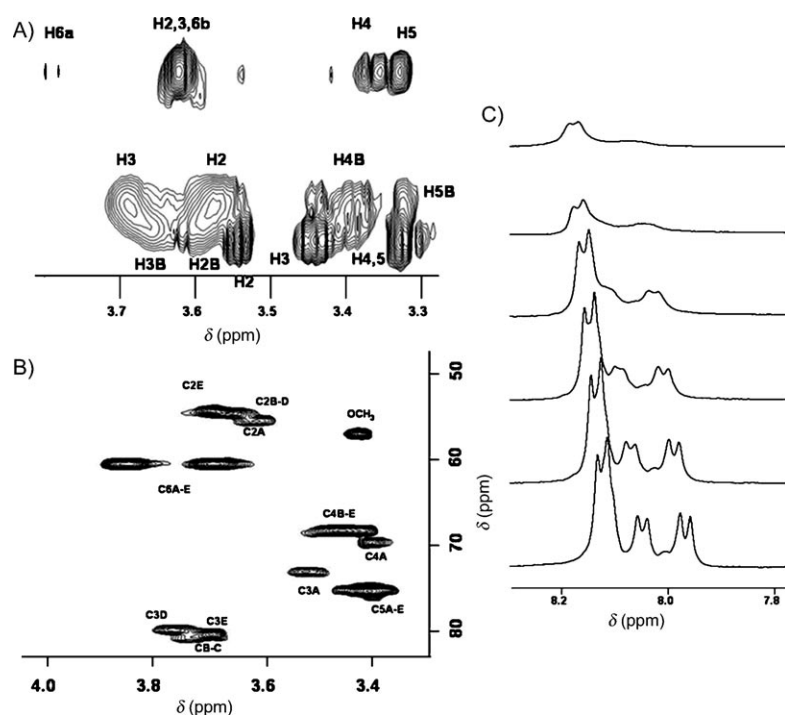


Figure 1. A) Sections of the NOESY experiment (300 ms, mixing time) from the anomeric region to the sugar resonances. B) Section of HSQC for the ring sugar protons, with the exception of the anomeric region. C) Variation of the shape of the amide protons of **1** with temperature.

Table 1. ¹H NMR spectroscopic chemical shifts [ppm] deduced for the pentasaccharide **1** in H₂O/D₂O at 298 K and 900 MHz.

Ring	Proton							
	H1	H2	H3	H4	H5	H6	NH	CH ₃
a	4.57	3.65	3.57	3.45	3.44	3.91, 3.73	8.02	1.99
b	4.54	3.69	3.78	3.49	3.43	3.91, 3.73	8.15	2.01
c	4.53	3.68	3.80	3.49	3.43	3.91, 3.73	8.15	2.02
d	4.52	3.71	3.82	3.49	3.43	3.91, 3.73	8.15	2.00
e	4.35	3.74	3.74	3.50	3.45	3.91, 3.73	8.10	2.05

anomeric proton produced one NOE contact with H-3 and H-5 of its own residue and H-3 at the residue to the other side of the glycosidic linkage. The intraresidual NOEs were employed as internal references for estimation of the proton–proton distances (Figure 1) and compared to those calculated from molecular mechanics (MM) and molecular dynamics (MD) calculations. Regarding the temperature coefficients for the amide protons, all of them oscillated between 8 and 10 ppbK⁻¹, which indicates that their degree of protection or participation in the intramolecular hydrogen bond is rather low. Indeed, they are in fast exchange with bulk solvent H₂O, and at 303 K, their signals are basically lost (Figure 1).

Molecular dynamics simulations: Different protocols were employed for accessing to the conformational and dynamic information of compound **1**. First, MD simulations (10 ns) were performed by using a continuum solvent model (GB/SA) and two different force fields, AMBER*^[12] and

MM3*^[13] as implemented in the MacroModel/MAESTRO^[14] package, and as described in the Experimental Section.

As the first step, the pentasaccharide was built by setting all the Φ and Ψ angles of every glycosidic linkage to 60:0°. Then, the resulting geometry was first extensively minimized by using conjugate gradients and then taken as the starting structure for the MD simulations by using AMBER* and MM3*. Typical trajectories are displayed in the Supporting Information. In all cases, no chair-to-chair or chair-to-boat interconversions were observed. Despite extensive minimization of the starting conformers, it is important to remark that, in both cases, although the average temperature was constant at around 300 K, important fluctuations (275–325 K) took place during the simulations, independently of the force field that

was employed. This situation is known to introduce artefacts in the dynamic properties of the system.^[15] Although the results should be considered as merely qualitative, it can be observed that, for both MM3* and AMBER* force fields (see also the Supporting Information), the trajectory remained in the corresponding low-energy region for the four glycosidic linkages, with basically no interconversions between conformers at these points. Therefore, according to these MD simulations, the *exo*-anomeric conformer^[16] at every glycosidic torsion was the most stable one, from a conformational point of view, together with the *syn-Ψ* conformer for the aglyconic linkage. Average angles oscillate between 40–65° for Φ and 0–40° for Ψ .

Several transitions between the possible orientations of the hydroxymethyl groups were also observed, especially between the *gg* and *gt* rotamers.^[17] Important differences were found for the torsion angle at the amide moiety. For the AMBER* simulations, an average H2-C2-N-H torsion of 240° was found, whereas for the MM3* protocol, the average value was 180°. These values were maintained even when the temperature of the simulation was set to 288, 303, or 313 K (6 ns simulation in each case with both force fields). In both cases, and considering the major conformation around the glycosidic linkage, there is basically no possibility of establishing inter-residual hydrogen bonds.

As further step, a 10 ns MD simulation in explicit water was also performed with the AMBER 9.0 force field, as described in the Experimental Section. The protocol included a 100 ps period in which the system was heated (100–303 K),

followed by a 100 ps equilibration at 303 K. Positional restraints were applied to the heavy atoms and were gradually lowered until no constrictions were applied. The unrestrained molecular dynamics simulation was continued during 10 ns at 303 K and 1 atm. Typical trajectories are displayed in Figure 2 and in the Supporting Information. The stability

Discussion

Correlation between the NMR spectroscopic and MD data:

According to the MD simulations, the glycosidic linkages adopt a well-defined conformation in the Φ/Ψ region around 60:0°. To demonstrate the existence of conformers defined by these values, the experimental NOE data can be analyzed. Indeed, for these geometries, close distances between H1 of a given residue and H3 of the following one should be expected, with interproton distances around 2.4 Å for every glycosidic linkage.

These contacts were indeed present in the NOE spectra, with strong intensities, in the range of those found for the intraresidual H1–H5 proton pair, which, according to the simulations, is defined by a very similar distance in a regular 4C_1 (D) chair. Thus, the experimental NMR spectroscopic results validated the accuracy of the MD simulations. Also, the global minimum generated from the MD simulations after extensive energy minimization cannot give any intraresidual hydrogen

tra, thus indicating their availability to chemical exchange processes. For the conformation around the amide region, the experimentally measured coupling constants $J_{\text{NH,H2}}$ (larger than 8 Hz) for all the residues are in agreement with major *anti*-type conformations for the corresponding protons, thus supporting the conclusions of the MM3* and AMBER 9.0 MD simulations. Also, the NHs gave NOE cross-peaks with the intraresidual H-1 proton (correlated with average MD HN–H1 distances of ca. 2.7 Å), which were stronger than those corresponding to the HN–H2 pairs (average MD HN–H2 distances of ca. 2.9 Å), again supporting a major *anti*-type geometry for the amide linkages.

In the obtained conformational families, the sugar glycosidic linkages can be described by major conformers in which Φ/Ψ are 60:0° with fluctuations around these values. Although the geometry is well defined, the pentasaccharide is not rigid at all, since the individual fluctuations at every linkage permits the existence of a large degree of accessible

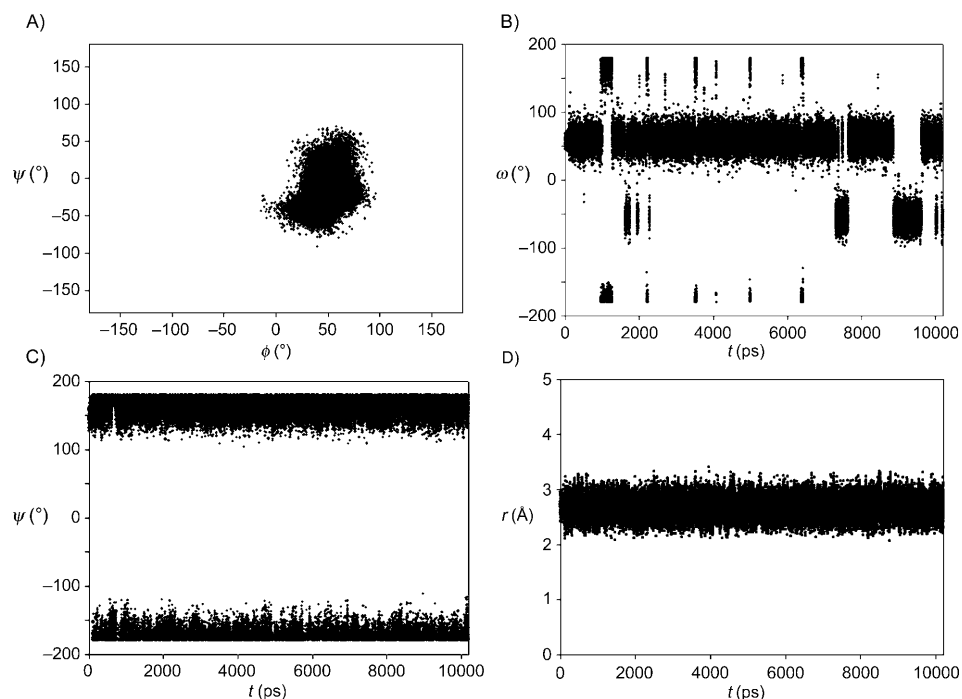


Figure 2. A) Φ/Ψ plot of the glycosidic torsions at the nonreducing end and its contiguous moiety of pentasaccharide **1** during the solvated MD simulation (10 ns, AMBER) at 300 K. B) Trajectories of the C4–C5–C6–O6 ω torsion angles at the nonreducing GlcNAc moiety during the 10 ns solvated simulation of **1** (AMBER, 300 K). C) Trajectory of the H2–C2–N–H torsion angle at the nonreducing end moiety during the 10 ns solvated simulation of **1** (AMBER, 300 K). D) Trajectory of the key inter-residual distance [Å] between the anomeric H-1 proton at the nonreducing end and the H-3 proton at the contiguous GlcNAc unit. The MD simulation spanned 10 ns with the AMBER force field at 300 K.

of the energy, pressure, and temperature was monitored along the trajectory and is given in different plots in the Supporting Information. The system was found to be fairly stable under the employed conditions. Again, the glycosidic linkages adopt the same conformation described above with fluctuations around 30–65° for Φ and 0–40° for Ψ (Figure 2). Also, transitions between the gg and gt rotamers of the hydroxymethyl groups were observed, with populations ranging between 60–80% for gg and 40–20% for gt, depending on the position within the pentasaccharide sequence (Figure 2). Nevertheless, it is possible that considerably longer simulation times^[18] (~100 ns) may be necessary to adequately sample the conformational space available to these molecules. Under these conditions in explicit water, the amide torsions adopted a major conformation with an *anti*-like H2–C2–N–H geometry for every residue, similar to that found in the MD simulation with the MM3* force field and the continuum solvent model (Figure 2).

conformational space. All the glycosidic torsions behave in an independent manner, with no correlations between their individual behavior and no contacts between residues that are more than one unit apart in the sequence. The possible conformations are fairly extended. In any case, the relative degree of flexibility permits these molecules to interact with a variety of receptors through similar or different presentation modes. Nevertheless, attending to the different situations, different entropic penalties will have to be paid for the interaction to take place. When the major conformer of this molecule is superimposed with that of the natural chitin analogue,^[19] it can be observed that the acetamide groups and the C6-hydroxymethyl groups occupy different spatial orientations. Also, the extension of the chain leads to subtle differences in the distances between the two reducing and nonreducing ends. These features may obviously imply distinct molecular recognition properties when the mimetic and the analogue interact with biomolecular receptors or specific enzymes.

Molecular recognition. The interaction with a model lectin and a model enzyme: WGA and chitinase: Since, in principle, the shape of the pentasaccharide is similar to that adopted by the similar penta-*N*-acetylated chitopentaose analogue, the possibility that the synthetic pentasaccharide could also be recognized by a chitin-binding lectin was analyzed. As a model carbohydrate-binding protein, wheat germ agglutinin was chosen, since it has been deeply studied and its recognition mode by chitin fragments has been firmly established.^[20]

Thus, NMR spectroscopic-based binding experiments were performed,^[21] at different concentrations with pentasaccharide/lectin ratios of 100:1, 40:1, and 20:1. The measurements were performed at 298 K and STD experiments^[22] were employed to detect binding and to deduce the binding epitope of the pentasaccharide (Figure 3).^[23]

Very neat results were obtained with the sample at a ratio L/P 20:1, which showed significant STD signals for the pro-

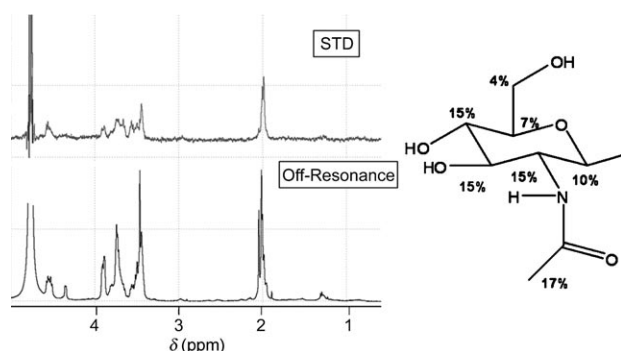


Figure 3. STD-NMR spectroscopic experiments on the WGA/pentasaccharide system. The number of scans was 128 ns, with 1 mM of the pentasaccharide at pH 7.02 (20 mM phosphate in D₂O). The ligand to protein ratio was 20:1. At the left-hand side, the STD on (above) and off-resonance (below) spectra. To the right-hand side, the observed absolute enhancements for the nonreducing end, which shows the maximum response after perturbation of the protein.

tons of the pentasaccharide, especially for those of the non-reducing end *N*-acetyl-D-glucosamine residue (e). For this e residue, the observed STD effects (Table 2) were more than double than those of the central residues (b–d) and three-fold those observed for the reducing end. Thus, the binding epitope was clearly characterized.

Table 2. STD percentages [%] observed on the different proton resonances of **1** upon saturation of the ¹H NMR spectrum at ca. $\delta = -1$ ppm (protein envelope).

Ring ^[a]	H1	H2	H3	H4	H5	H6	COCH ₃	OCH ₃
ring a nonred	10	15	15	15	7	4	17	
ring b	8	5	7	6	7	4	8	
ring c+d	12	– ^[b]	14	12	14	8	6	
ring d	6	– ^[b]	7	6	7	4	3	
ring e red	5	– ^[b]	4	– ^[b]	– ^[b]	– ^[b]	2	2

[a] See Figure 3. [b] Not detected.

Finally, trNOE experiments were also performed to characterize the bound geometry.^[24] Very strong negative cross-peaks were observed for the pentasaccharide at 298 K and 500 MHz, and even when using a mixing time of only 75 ms. This fact is a clear indication of binding, because the NOESY spectrum of the free pentasaccharide at 298 K at this mixing time was basically devoid of cross-peaks. No new peaks were observed in the trNOESY spectrum (Figure 4), when compared with the NOESYs recorded for the saccharide in the free state at 800 MHz, which indicates that no lectin-induced conformational variations were taking place in the pentasaccharide structure. Thus, the major conformation in solution is that bound by the lectin.

To rationalize the interaction on the molecular level, the low-energy conformer of **1**, as deduced by the NMR spectroscopic experiments, was docked into the different WGA binding sites^[25] by using two different docking programs, AutoDock^[26] and Glide.^[27] Four hevein domains are known in the lectin.^[25] The binding sites for chitooligosaccharides are very similar in the different domains and are defined by one Ser residue (residue at relative position 62, from the N terminus), which provides hydrogen bonds to the carbonyl group of one acetamide residue, two aromatic residues (i.e., residues Tyr64 and His66), which make stacking interactions to two consecutive GlcNAc units, and one tyrosine moiety (Tyr 73), which provides stabilizing van der Waals interactions to the acetamide methyl group and one additional hydrogen bond to one sugar hydroxyl group (Figure 5).^[28] The docking protocol (see the Experimental Section) permitted the deduction that the N terminus was nicely accommodated in the protein binding site, at Tyr73. The second and third units provided minor contacts with the protein, whereas the fourth one and the reducing end were basically in contact with the solvent. It has been demonstrated that chitooligosaccharides may adopt different orientations at the binding sites of hevein domains. In this case, given the different orientations of the acetamide moieties for the GlcNAc residues in the β -1→3 versus the β -1→4 linkages, Glide only led to

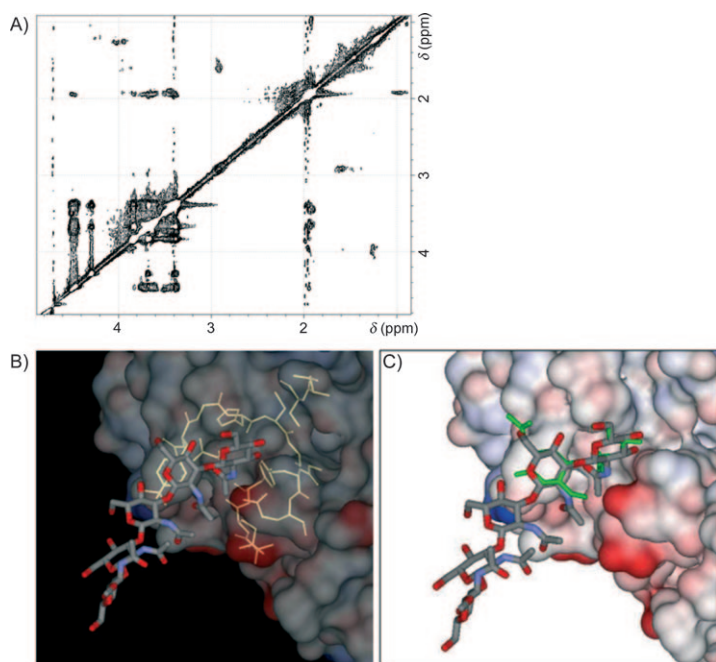


Figure 4. A) Tr NOESY spectrum (200 ms mixing time) of **1** in the presence of WGA, a model lectin. Negative cross-peaks are observed, which indicate lectin binding. In the views below, the recognition mode of the chitin mimetic by the lectin is shown. B) Major contacts are observed for the nonreducing end (as also assessed by the NMR STD experiments), followed by the second residue. Only marginal contacts are observed for the third residue, whereas the fourth and fifth ones are in contact with the solution. C) Pentasaccharide **1** is superimposed with chitobiose, by using the nonreducing end. The different orientations of the acetamide and C6-hydroxymethyl groups are evidenced.

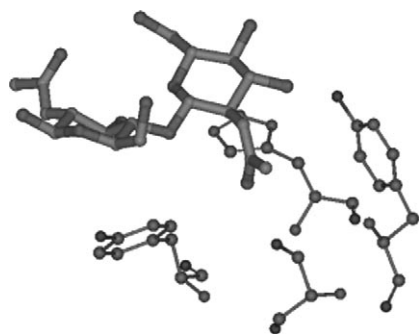


Figure 5. Typical binding site of chitooligosaccharides at hevein domains. The case for one of the binding sites of WGA is shown. The binding is defined by Ser62, which provides a hydrogen bond to the carbonyl group of one acetamide residue, residues Tyr64 and His66, which make stacking interactions to the two consecutive GlcNAc units, and Tyr73, which provides stabilizing van der Waals interactions to the acetamide methyl group and one additional hydrogen bond to one sugar hydroxyl group.^[28]

one major docking pose. The analogous analysis with AutoDock provided the same results. Thus, the key conclusion is that the docking analysis was in accordance with the NMR spectroscopic-derived observations. The studies described herein indicate that the chemical modifications from $\beta(1-4)$ to $\beta(1-3)$ influence the spatial disposition of the sugar chain,

but keeping the overall shape and somehow, the molecular recognition abilities.

Furthermore, we also explored the possibility of the enzymatic hydrolysis of this synthetic pentasaccharide by an *N*-acetyl glycosaminidase enzyme. NMR spectroscopic experiments were carried out on a pentasaccharide sample, by using the chitinase from *Streptomyces Griseus*. This enzyme was employed since it is able to readily hydrolyze $\beta(1-4)$ linkages in natural chitin oligosaccharides. The 1D ^1H NMR spectroscopic experiments were performed in buffer phosphate D_2O (50 mM pH 6 at 298 K) with a sugar to enzyme molar ratio of 20:1. After two hours, the NMR spectra did not show any variation of the intensity of the sugar peaks, especially at the structural reporter anomeric region. The nonreducing-end proton kept the same intensity throughout the whole two-hour experiment, and also after 24 h. A completely different behavior was observed for the reference experiments with the natural chitopentaose substrate. Thus, the change from $\beta(1-4)$ to a $\beta(1-3)$ linkage precludes the hydrolysis, at least for this particular enzyme. However, slight line broadening was observed for the signals of compound **1** and also STD experiments gave rise to several signals at the sugar region, thus assessing that interactions between the synthetic pentasaccharide **1** with the enzyme were taking place (Figure 6). DOSY experiments allowed the confirmation that **1** is not degraded. Although merely speculative, the observed interaction throughout the line broadening of the NMR spectroscopic resonance signals and the STD enhancements could arise from interactions at the chitin binding domain of the enzyme and not at the intrinsic catalytic site. Indeed, the inhibitory power of the synthetic pentasaccharide to avoid chitopentaose degradation was very weak, in the millimolar range.

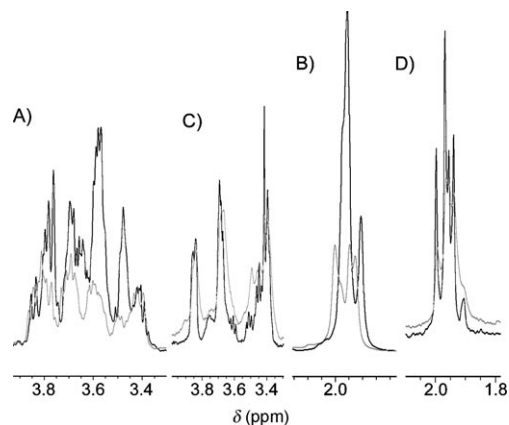


Figure 6. Hydrolysis of the natural penta-*N*-acetyl chitopentaose by the chitinase enzyme. Clear variations at the sugar region (A) and at the acetate methyl region (B) are observed, verifying hydrolysis. In contrast, only line broadening is observed for pentasaccharide **1** in the presence of the chitinase, both for the sugar (C) and methyl region (D). The data indicate ligand binding to the protein, but not hydrolysis.

Experimental Section

Synthesis: General methods: Optical rotations were measured at $20 \pm 2^\circ\text{C}$ with a Perkin–Elmer Model 241 digital polarimeter, by using a 10 cm, 1 mL cell. Chemical ionization (CI) and Fast Atom Bombardment (FAB) mass spectra were obtained with a JMS-700 spectrometer. Electrospray ionization (ESI) mass spectra were recorded with a Q-TOF1 (Micromass) time-of-flight mass spectrometer. ^1H NMR spectra were recorded with a Bruker DRX 400 spectrometer at ambient temperature. Assignments were aided by COSY experiments. ^{13}C NMR spectra were recorded at 100.6 MHz with a Bruker DRX 400 for solutions in CDCl_3 or D_2O . CDCl_3 was adopting a peak at $\delta = 77.00$ ppm (for the central line of CDCl_3). Spectra in water were referenced by using DSS (dodecyl sodium sulfate) as external standard. Assignments were aided by a J-mod technique and proton–carbon correlation. Reactions were monitored by TLC on a precoated plate of silica gel (60F₂₅₄, layer thickness 0.2 mm, E. Merck, Darmstadt, Germany) and detection by charring with sulfuric acid. Flash-column chromatography was performed on silica gel 60 (230–400 mesh, E. Merck).

Methyl (4,6-*O*-benzylidene-2-deoxy-2-phthalimido- β -D-glucopyranosyl)-(1 \rightarrow 3)-(4,6-*O*-benzylidene-2-deoxy-2-phthalimido- β -D-glucopyranosyl)-(1 \rightarrow 3)-4,6-*O*-benzylidene-2-deoxy-2-phthalimido- β -D-glucopyranoside (2): Magnesium (1.68 g, 0.07 mol) was added to dry methanol (50 mL); then a few iodine crystals were added into the solution. The mixture was refluxed for 2 h to give a $\text{Mg}(\text{OMe})_2$ solution. The freshly prepared $\text{Mg}(\text{OMe})_2$ solution (12 mL) was then added to a solution of **3** (383 mg, 0.316 mmol) in dry dichloromethane (12 mL). After the reaction mixture had been stirred for 48 h at room temperature under argon, TLC showed completion of the reaction. The mixture was neutralized to pH 7 with acetic acid, filtered, and concentrated. The residue was dissolved in dichloromethane and washed with water, dried with MgSO_4 , and concentrated. The residue was flash-chromatographed with silica gel (dichloromethane/ethyl acetate 20:1) to give **2** (329 mg, 89%) as a white powder: $R_f = 0.38$ (cyclohexane/ethyl acetate 1:2); $[\alpha]_D = -38$ ($c = 1.0$ in chloroform); ^1H NMR (400 MHz, CDCl_3): $\delta = 5.52$ (s, 1H; PhCH), 5.47 (s, 1H; PhCH), 5.42 (s, 1H; PhCH), 5.21 (d, 1H, $J = 8.40$ Hz; H-1''), 5.10, 4.85 (2d, 2H, $J = 8.5$, 8.4 Hz; H-1, H-1'), 4.82, 4.66 (2dd, 2H, $J_{2,3} = 10.37$, $J_{3,4} = 9.10$, $J_{2,3'} = 10.30$, $J_{3,4'} = 8.90$ Hz; H-3, H-3'), 4.27 (dd, 1H, $J_{2',3'} = 10.25$, $J_{3',4'} = 9.78$ Hz; H-3''), 4.35, 4.20 (2dd, 2H, $J_{5,6b} = 4.81$, $J_{6a,6b} = 10.45$, $J_{5,6b} = 4.80$, $J_{6a,6b} = 10.44$ Hz; H-6b, H-6'b), 4.14, 4.08 (2dd, 2H, $J_{1,2} = 8.45$, $J_{2,3} = 8.51$, $J_{1,2} = 8.32$, $J_{2,3'} = 10.30$ Hz; H-2, H-2'), 4.11 (dd, 1H, $J_{6'a,6'b} = 10.40$, $J_{5',6'b} = 4.53$ Hz; H-6''b), 4.03 (dd, 1H, $J_{1',2'} = 8.45$, $J_{2',3'} = 8.39$ Hz; H-2''), 3.81, 3.72 (2t, 2H, $J_{5,6a} = J_{6a,6b} = 10.25$, $J_{5',6'a} = J_{6'a,6'b} = 10.17$ Hz; H-6a, H-6'a), 3.65 (t, 2H, $J = 9.19$, 9.01 Hz; H-4, H-4'), 3.57 (t, 1H, $J = 10.7$ Hz; H-6''a), 3.55, 3.39 (2m, 2H; H-5, H-5'), 3.39 (dd, 1H, $J = 9.13$, 9.10 Hz; H-4''), 3.30 (s, 3H; OCH₃), 3.27 (m, 1H; H-5''), 2.16 ppm (brs, 1H; OH); ^{13}C NMR (100.6 MHz, CDCl_3): $\delta = 137.21$, 137.11, 136.91, 131.37, 131.15, 130.92, (arom. C), 133.90, 133.62, 129.29, 129.27, 129.07, 129.01, 128.28, 128.24, 128.20, 128.15, 126.23, 126.04, 125.99, 123.48, 123.19, 123.07 (arom. CH), 101.76, 101.11 ($3 \times \text{PhCH}$), 99.65, 97.43, 97.17 (C-1, C-1', C-1''), 81.79, 79.90, 79.78 (C-4, C-4', C-4''), 74.22, 73.93, 68.34 (C-3, C-3', C-3''), 68.62, 68.54 (C-6, C-6', C-6''), 66.29, 66.07, 65.72 (C-5, C-5', C-5''), 56.84 (OCH₃), 56.01, 55.58, 55.54 ppm (C-2, C-2', C-2''); HRMS (CI⁺): m/z : calcd for $\text{C}_{64}\text{H}_{55}\text{O}_{19}\text{N}_3\text{Na}$: 1192.3327 [$M+\text{Na}$]⁺; found: 1192.3298.

3-*O*-Acetyl-4,6-*O*-benzylidene-2-deoxy-2-phthalimido-D-glucopyranose (5): A solution of compound **4** (3 g, 5.64 mmol, 1 equiv), THF (18 mL), and water (3.6 mL) was stirred for 30 min at room temperature. Then the reaction mixture was cooled to 0°C and a mixture of HgO (1.8 g, 8.42 mmol, 1.5 equiv), THF (8 mL), and $\text{BF}_3 \cdot \text{Et}_2\text{O}$ (1.4 mL, 2.0 equiv) was added slowly. After stirring at room temperature for 32 h, the reaction mixture was neutralized with Et_3N and concentrated. The residue was dissolved in dichloromethane, washed with saturated aqueous NaHCO_3 solution, aqueous KI solution (10%), water, and saturated brine. The resulting mixture was dried with MgSO_4 and concentrated. The residue was flash-chromatographed with silica gel (dichloromethane/ethyl acetate 15:1, Et_3N , 0.1%), to give **5** (1.39 g, 56%), which was engaged directly to the next reaction.

3-*O*-Acetyl-4,6-*O*-benzylidene-2-deoxy-2-phthalimido- β -D-glucopyranosyl trichloroacetimidate (6): A mixture of **5** (690 mg, 1.57 mmol) and 4 Å molecular sieves (2.16 g) in dry dichloromethane (28 mL) was stirred at room temperature for 30 min under argon. After the reaction mixture had been cooled to 0°C , trichloroacetonitrile (2.16 mL) and DBU (279 μL) were added dropwise. The mixture was stirred at 0°C for 5 h, then filtered through a Celite bed. After concentration, the residue was purified by flash chromatography with silica gel (dichloromethane/ethyl acetate 40:1 with 0.1% triethylamine) to give the **6** as a white powder (610 mg, 67%). $R_f = 0.50$ (cyclohexane/ethyl acetate 1.5:1); $[\alpha]_D = -24$ ($c = 1$ in chloroform); ^1H NMR (400 MHz, CDCl_3): $\delta = 7.90$ –7.20 (m, 9H; arom.), 6.75 (d, 1H, $J_{1,2} = 8.78$ Hz; H-1), 6.05 (dd, 1H, $J_{2,3} = 9.29$, $J_{3,4} = 10.04$ Hz; H-3), 5.61 (s, 1H; PhCH), 4.64 (dd, 1H, $J_{1,2} = 8.79$, $J_{2,3} = 10.27$ Hz; H-2), 4.53 (dd, 1H, $J_{5,6b} = 4.17$, $J_{6a,6b} = 9.91$ Hz; H-6a), 4.03–3.89 (m, 3H; H-4, H-5, H-6b), 1.96 ppm (s, 3H; OAc); ^{13}C NMR (100.6 MHz, CDCl_3): $\delta = 170.14$ (C=O, Ac), 167.49, 163.62 (C=O, NPhth), 160.55 (C=NH), 136.62, 131.13, (arom. C), 134.41, 129.23, 128.24, 126.22, 123.64 (arom. CH), 101.74 (PhCH), 93.94 (C-1), 78.78 (C-4), 69.38 (C-3), 68.37 (C-6), 66.94 (C-5), 54.21 (C-2), 20.53 ppm ($\text{CH}_3\text{C}=\text{O}$); HRMS (FAB⁺): m/z : calcd for $\text{C}_{25}\text{H}_{21}\text{O}_8\text{N}_2\text{Cl}_3\text{K}$: 621.0001 [$M+\text{K}$]⁺; found: 621.0016.

Phenyl 3-*O*-(3-*O*-acetyl-4,6-*O*-benzylidene-2-deoxy-2-phthalimido- β -D-glucopyranosyl)-4,6-*O*-benzylidene-2-deoxy-2-phthalimido-1-thio- β -D-glucopyranoside (8): A solution of **6** (360 mg, 0.62 mmol, 1.2 equiv) and **7** (250 mg, 0.52 mmol, 1 equiv) in dry dichloromethane (2.5 mL) was stirred with ground 4 Å (896 mg) molecular sieves for 40 min at room temperature under an argon atmosphere. TMSOTf (110 μL , 0.52 mmol, 1 equiv) was added dropwise at 0°C , and the mixture was stirred at that temperature for 3 h. The reaction mixture was then filtered through Celite and the solid was washed with dichloromethane. The filtrate was washed with saturated aqueous NaHCO_3 solution and then with water, dried over MgSO_4 , and concentrated. The residue was flash-chromatographed from a column of silica gel (cyclohexane/ethyl acetate 2:1) to give **8** (420 mg, 79%). $R_f = 0.39$ (cyclohexane/ethyl acetate 1.5:1); $[\alpha]_D = +29$ ($c = 1$ in chloroform); ^1H NMR (400 MHz, CDCl_3): $\delta = 7.8$ –7.20 (m, 23H; arom.), 5.62 (t, 1H, $J_{2,3} = J_{3,4} = 9.73$ Hz; H-3'), 5.61, 5.45 (2s, 2H; $2 \times \text{PhCH}$), 5.60, 5.47 (2d, 2H, $J = 8.54$, 8.05 Hz; H-1, H-1'), 4.89 (dd, 1H, $J_{2,3} = 8.88$, $J_{3,4} = 9.84$ Hz; H-3), 4.40 (dd, 1H, $J_{5,6a} = 4.7$, $J_{6a,6b} = 10.47$ Hz; H-6a), 4.35 (dd, 1H; H-2), 4.21 (dd, 1H; H-2'), 4.12 (dd, 1H; $J_{5',6'a} = 4.81$, $J_{6'a,6'b} = 10.47$ Hz; H-6'a), 3.87 (t, 1H, $J = 10.10$ Hz; H-6b), 3.78 (t, 1H, $J = 9.05$ Hz; H-4), 3.70 (m, 1H; H-5), 3.67 (t, 2H, $J = 9.65$ Hz; H-4', H-6'b), 3.48 (m, 1H; H-5'), 1.77 ppm (s, 3H; OAc); ^{13}C NMR (100.6 MHz, CDCl_3): $\delta = 170.00$ (C=O, Ac), 137.02, 136.85, 131.68 (arom. C), 134.08, 133.93, 132.31, 129.22, 129.09, 128.89, 128.29, 128.15, 128.02, 126.23, 126.00, 123.26 (arom. CH), 101.56, 101.32, 97.58 ($2 \times \text{PhCH}$, C-1'), 84.72 (C-1), 80.11, 78.82 (C-4, C-4'), 75.81, 69.75 (C-3, C-3'), 70.51, 65.90 (C-5, C-5'), 68.56, 68.50 (C-6, C-6'), 55.64, 54.54 (C-2, C-2'), 20.35 ppm ($\text{CH}_3\text{C}=\text{O}$); HRMS (FAB⁺): m/z : calcd for $\text{C}_{50}\text{H}_{42}\text{O}_{13}\text{N}_2\text{SNa}$: 933.2305 [$M+\text{Na}$]⁺; found: 933.2318.

Methyl (3-*O*-acetyl-4,6-*O*-benzylidene-2-deoxy-2-phthalimido- β -D-glucopyranosyl)-(1 \rightarrow 3)-(4,6-*O*-benzylidene-2-deoxy-2-phthalimido- β -D-glucopyranosyl)-(1 \rightarrow 3)-(4,6-*O*-benzylidene-2-deoxy-2-phthalimido- β -D-glucopyranosyl)-(1 \rightarrow 3)-4,6-*O*-benzylidene-2-deoxy-2-phthalimido- β -D-glucopyranoside (9): A mixture of compound **2** (312 mg, 0.267 mmol, 1 equiv), **8** (243 mg, 0.267 mmol, 1 equiv), 4 Å powered molecular sieves (1.2 g) and dry dichloromethane (17 mL) was stirred at room temperature for 30 min under argon. NIS (140 mg, 0.61 mmol, 2.3 equiv) was added and the reaction mixture was cooled to -30°C ; then triflic acid (2.36 μL , 0.027 mmol, 0.1 equiv) was introduced by dilution in dichloromethane. After stirring at -30°C for 4 h, the reaction mixture was neutralized with Et_3N , filtered through a Celite bed, washed with water, saturated aqueous thiosulfate solution, and saturated brine, dried with MgSO_4 , and concentrated. The residue was flash-chromatographed with silica gel (cyclohexane/acetone 4:3), to give **9** (472 mg, 90%) as an amorphous white powder. $R_f = 0.32$ (cyclohexane/acetone 1:1). $[\alpha]_D = -49$ ($c = 1$ in chloroform); ^1H NMR (400 MHz, CDCl_3): $\delta = 7.80$ –7.10 (m, 45H; arom.), 5.49 (t, 1H, $J = 9.8$ Hz; H-3e), 5.49 (s, 1H; PhCH), 5.41 (s, 1H; PhCH), 5.40 (s, 1H; PhCH), 5.38 (s, 1H; PhCH), 5.37 (s, 1H; PhCH), 5.35 (d, 1H, $J = 8.35$ Hz; H-1e), 4.99, 4.85, 4.82, 4.78 (4d, 4H, $J = 8.37$, 8.33, 8.23, 7.39 Hz;

H-1a, H-1b, H-1c, H-1d), 4.79 (m, 1H; H-3c), 4.57, 4.53, 4.49 (3dd, 3H, $J_{2a,3a}=9.07$, $J_{3a,4a}=10.3$, $J_{2b,3b}=9.07$, $J_{3b,4b}=10.39$, $J_{2d,3d}=9.12$, $J_{3d,4d}=10.21$ Hz; H-3a, H-3b, H-3d), 4.33 (dd, 1H, $J_{5c,6c}=4.74$, $J_{6c,6'c}=10.46$ Hz; H-6c), 4.18, 4.13 (3dd, 3H, $J_{5a,6a}=4.72$, $J_{6a,6'a}=10.3$, $J_{5b,6b}=5.34$, $J_{6b,6'b}=9.4$, $J_{5d,6d}=5.34$, $J_{6d,6'd}=9.4$ Hz; H-6a, H-6b, H-6d), 4.07-3.94 (m, 5H; H-6e, H-2a, H-2b, H-2c, H-2e), 3.90 (dd, 1H, $J_{1d,2d}=8.37$, $J_{2d,3d}=10.37$ Hz; H-2d), 3.79 (t, 1H, $J=10.11$ Hz; H-6'c), 3.70-3.43 (m, 10H; H-6'a, H-6'b, H-6'd, H-6'e, H-4a, H-4b, H-4c, H-4d, H-4e, H-5c), 3.30 (ddd, 2H; H-5d, H-5e), 3.28 (s, 3H; OCH₃), 3.25-3.15 (m, 2H; H-5a, H-5b), 1.70 ppm (s, 3H; OAc); ¹³C NMR (100.6 MHz, CDCl₃): $\delta=169.84$ (C=O, Ac), 167.18, 167.15, 167.01 (C=O, NPhth), 137.11, 137.08, 137.04, 137.02, 136.79, 131.26, 130.81, 130.72 (arom. C), 133.89, 133.66, 133.62, 133.46, 129.01, 128.96, 128.89, 128.87, 128.14, 128.10, 128.07, 126.14, 125.96, 125.91, 125.88 (arom. CH), 101.41, 101.03, 100.95, 100.87 (5 \times PhCH), 99.60, 97.32, 96.78 (C-1a, C-1b, C-1c, C-1d, C-1e), 79.75, 79.72, 79.32, 79.28, 78.67 (C-4a, C-4b, C-4c, C-4d, C-4e), 74.09, 73.71, 73.15, 73.06, 69.59 (C-3a, C-3b, C-3c, C-3d, C-3e), 68.43 (C-6a, C-6b, C-6c, C-6d, C-6e), 66.20, 65.99, 65.86, 65.75, 65.63 (C-5a, C-5b, C-5c, C-5d, C-5e), 56.79 (OCH₃), 55.63, 55.53, 55.49, 55.42, 55.34 (C-2a, C-2b, C-2c, C-2d, C-2e), 20.24 ppm (CH₃C=O); HRMS (FAB⁺): *m/z*: calcd for C₁₀₈H₉₁O₃₂N₅Na: 1992.5545 [M+Na]⁺; found: 1992.5571.

Methyl (3-O-acetyl-2-deoxy-2-phthalimido- β -D-glucopyranosyl)-(1 \rightarrow 3)-(2-deoxy-2-phthalimido- β -D-glucopyranosyl)-(1 \rightarrow 3)-(2-deoxy-2-phthalimido- β -D-glucopyranosyl)-(1 \rightarrow 3)-(2-deoxy-2-phthalimido- β -D-glucopyranosyl)-(1 \rightarrow 3)-2-deoxy-2-phthalimido- β -D-glucopyranoside (10-1) and methyl (2-deoxy-2-phthalimido- β -D-glucopyranosyl)-(1 \rightarrow 3)-(2-deoxy-2-phthalimido- β -D-glucopyranosyl)-(1 \rightarrow 3)-(2-deoxy-2-phthalimido- β -D-glucopyranosyl)-(1 \rightarrow 3)-(2-deoxy-2-phthalimido- β -D-glucopyranosyl)-(1 \rightarrow 3)-2-deoxy-2-phthalimido- β -D-glucopyranoside (10-2): *p*-Toluenesulfonic acid (2.3 mg) was added to a solution of compound **9** (235 mg, 0.12 mmol) in THF (2.8 mL) and methanol (11.9 mL), the mixture was then stirred and heated at 55 °C for 24 h. After neutralization with saturated aqueous NaHCO₃ solution, the mixture was dried over MgSO₄ and concentrated. The residue was flash-chromatographed by using a column of silica gel (dichloromethane/methanol 7:1). Compound **10-1** eluted first (122 mg, 66%; MS (FAB⁺): *m/z*: C₇₃H₇₁O₃₂N₅Na: 1552.32 [M+Na]⁺) followed by compound **10-2**, which eluted second (38 mg, 21%; MS (FAB⁺): *m/z*: C₇₁H₆₉O₃₁N₅Na: 1510.60 [M+Na]⁺).

Methyl (2-acetamido-2-deoxy- β -D-glucopyranosyl)-(1 \rightarrow 3)-(2-acetamido-2-deoxy- β -D-glucopyranosyl)-(1 \rightarrow 3)-(2-acetamido-2-deoxy- β -D-glucopyranosyl)-(1 \rightarrow 3)-2-acetamido-2-deoxy- β -D-glucopyranoside (1): Hydrazine hydrate (0.25 mL) and water (0.25 mL) were added to a stirred solution of compound **10-1** (20 mg, 0.013 mmol) in ethanol (4.2 mL), and the mixture was refluxed for 12 h at 80 °C. The reaction mixture was concentrated and the residue was used in the next reaction directly.

Water (0.4 mL), methanol (3.6 mL), and NaHCO₃ (300 mg, 7.5 equiv) were added to the residue obtained above. The mixture was stirred at 0 °C and acetic anhydride (1 mL) was added dropwise. After stirring at room temperature for 4 h, the mixture was evaporated under reduced pressure. The residue was chromatographed by a column of Sephadex G25 (distilled water) to give the pentasaccharide **1** (6.5 mg, 48% for two steps) as an amorphous white powder. $R_f=0.21$ (ethyl acetate/isopropanol/H₂O 1:1:1); $[\alpha]_D^{20}=-10$ ($c=0.8$ in H₂O); ¹H NMR (400 MHz, D₂O): $\delta=4.57$, 4.56, 4.54, 4.52, 4.35 (5d, 5H, $J=8.2$, 7.2, 8.4, 8.7, 8.3 Hz; H-1a, H-1b, H-1c, H-1d, H-1e), 3.47 (s, 3H; OCH₃), 2.05, 2.02, 2.01, 1.99 ppm (5s, 15H; CH₃, 5 \times Ac); ¹³C NMR (100.6 MHz, D₂O): $\delta=174.88$, 174.52, 174.25, 174.22, 174.15 (C=O, 5 \times Ac), 102.57, 101.34, 101.19, 100.92, 100.89 (5 \times C-1), 81.22, 80.77, 80.36, 80.17, 76.12, 75.73, 75.63, 75.58, 75.56, 73.55, 70.15, 68.86, 68.77, 68.67, 68.66 (5 \times C-3, 5 \times C-4, 5 \times C-5), 61.12, 61.00, 60.94 (5 \times C-6), 57.55 (OMe), 56.02, 55.23, 55.22, 55.01, 54.83 (5 \times C-2), 22.86, 22.84, 22.76, 22.73, 22.63 ppm (CH₃, 5 \times Ac); MS (FAB⁺): *m/z*: 1086.37 [M+K]⁺; HRMS (ESI⁺): *m/z*: calcd for C₆₁H₆₉O₂₆N₅Na: 1070.4128 [M+Na]⁺; found: 1070.4175.

By using the same procedure, compound **10-2** was deprotected and N-acetylated to also afford the target **1**.

NMR spectroscopy: For the NMR spectroscopic measurements, the pentasaccharide (~2 mg) was dissolved in D₂O (0.5 mL, phosphate buffer,

pH 5.7). Spectra in H₂O 85/D₂O 15% (0.5 mL) were also recorded to look at the exchangeable amide protons.

2D-NOESY and TOCSY spectra were obtained by using the standard pulse sequences provided by the manufacturer in different spectrometers: BRUKER AVANCE spectrometer operating at a frequency of 800 MHz and a VARIAN NMR spectrometer operating at a frequency of 900 MHz. NOESY spectra were collected with mixing times ranging between 60 and 300 ms at 278, 288, 298 and 308 K. For DOSY experiments, the samples were prepared in D₂O and the standard BRUKER DOSY protocol was used at 298 K on an AVANCE 500 MHz equipped with a broad-band z-gradient probe. Thirty-two 1D ¹H spectra were collected with a gradient duration of $\delta=2$ ms and an echo delay of $\Delta=100$ ms. Acquisition times of 8–15 min (8–16 scans) were required for the samples. The ledppg2s pulse sequence, with stimulated echo, longitudinal eddy current compensation, bipolar gradient pulses, and two spoil gradients, was run with a linear gradient (53.5 G cm⁻¹) stepped between 2 and 95%. The 1D ¹H spectra were processed and automatically baseline corrected. The diffusion dimension, zero-filled to 1k, was exponentially fitted according to preset windows for the diffusion dimension ($-8.5 < \log D < -10.0$).

Interaction studies with WGA lectin: Commercial WGA was purchased from Sigma. The binding of the pentasaccharide was evaluated by STD experiments performed with 20:1, 40:1, and 100:1 molar ratios of the sugar/WGA mixture. The concentration of the protein was ca. 150 μ M. A series of Gaussian-shaped pulses of 50 ms each was employed with a total saturation time for the protein envelope of 2 s and a maximum B1 field strength of 60 Hz. An off-resonance frequency of $\delta=40$ ppm and on-resonance frequency of $\delta=-1.0$ ppm (protein aliphatic signals region) were applied.

The exchange transferred NOE experiments (trNOE) were performed by using regular 2D-NOESY experiments. Measurements were done with a freshly prepared ligand/lectin mixture, with mixing times of 75 and 150 ms, by using a 20:1 molar ratio of ligand/protein. A concentration of 1 mM of the ligand was employed. No purging spin-lock period was employed to remove the NMR spectroscopic signals of the macromolecule background. Strong negative NOE cross-peaks were observed, in contrast to the free state, which indicates binding of the sugars to the lectin preparation.

Interaction studies with the chitinase: Commercial chitinase (from *Streptomyces Griseus*) was purchased from Sigma (C6137-5UN), and its interaction with pentasaccharide **1** was monitored by 1D ¹H NMR spectroscopic experiments. NMR spectra were performed in deuterated buffer phosphate (50 mM, pH 6) at 298 K, the concentration of the pentasaccharide was 1 mM, and the ratio between the sugar and enzyme was 20:1. ¹H NMR spectroscopic experiments were recorded for 2 h (for the initial 30 min, the ¹H NMR spectroscopic experiments were recorded every 2 min; then at regular intervals of 5 min for 1.30 h) after the addition of the enzyme. One additional experiment was carried out 24 h later. STD experiments were recorded on the same samples, a series of Gaussian-shaped pulses of 50 ms each was employed with a total saturation time for the protein envelope of 2 s and a maximum B1 field strength of 60 Hz. An off-resonance frequency of $\delta=40$ ppm and an on resonance frequency of $\delta=-1.0$ ppm (protein aliphatic signals region) were applied. The DOSY experiments were performed with the standard BRUKER DOSY protocol at 298 K on an AVANCE 600 MHz, equipped with a broad-band z-gradient probe. No change in the diffusion coefficient of the sample was observed after 24 h.

Molecular dynamics simulations

In vacuo: As the first step, pentasaccharide **1** was built by setting all the Φ and Ψ angles of every glycosidic linkage to 60:0°. Then, the resulting geometry was extensively minimized by using conjugate gradients and then taken as the starting structure for the MD simulations by using AMBER* and MM3* force fields. The desired temperature (300 K) was obtained by raising the temperature from 0 to 300 K in 10 K increments every ps. This heating period was followed by a 170 ps equilibration period and a 10 ns trajectory. The temperature was controlled during the equilibration and simulation periods by coupling to a temperature bath, with an exponential decay constant of 0.1 ps. During the equilibration

period, the velocities were scaled when the difference between the actual and the required temperature was higher than 10°. Trajectory frames were saved every 5 ps.

In explicit solvent: A 10 ns MD simulation was carried out by using the AMBER 9 package.^[29] Initial structures were built by using Sybyl 7.3 and their initial coordinates were based on geometries taken from the previous results obtained in vacuum. Partial atomic charges were obtained by using the restricted electrostatic potential (RESP) method.^[30] For this purpose all molecules were first subjected to a single-point calculation with the HF/6-31G* basis set by using Gaussian 03.^[31] Glycam 04 atomic types were assigned to the carbohydrate moiety.^[32] Compound **1** was placed in a 10 Å depth truncated octahedral box of explicit TIP3P waters. The equilibration phase consisted of energy minimization of the solvent followed by an energy minimization of the entire system without restraints. The system was then heated up to 288 K during 100 ps, followed by 100 ps at constant temperature and constant pressure of 1 atm. The unrestrained MD simulation was continued during 10 ns under a constant pressure of 1 atm. and constant temperature of 288 K controlled by the Langevin thermostat with a collision frequency of 1.0 ps⁻¹. During the simulation, the SHAKE algorithm^[33] was applied to all hydrogen atoms. A cut-off of 10 Å for all nonbonded interactions was adopted. An integration time step of 2 fs was employed and periodic boundary conditions were applied throughout. The particle mesh Ewald (PME) method was used to compute long-range electrostatic interactions.^[34] Minimization, equilibration, and production phases were carried out by the SANDER module, whereas the analyses of the simulations were performed by using the Ptraj module of AMBER 9. The visualization of the trajectories was performed by using VMD software. Data processing and a 2D plot were created by using Scilab and Sigmaplot software.

Docking calculations: The major conformer of the pentasaccharide in the free state (as deduced by the combined NMR spectroscopic and molecular modeling approach) was docked into the carbohydrate binding sites of WGA (PDB code 2UVO). Indeed, this conformer was used as input geometry for the docking calculations with AutoDock 3.0^[26] and Glide.^[27] The ligand charges were those estimated above. For the docking studies with AutoDock, the multiple Lamarckian Genetic Algorithm was chosen. Only local searches were performed centered in the experimental chitin-specific binding sites. Grids of probe atom interaction energies and electrostatic potential were generated by the AutoGrid program present in AutoDock 3.0. A grid spacing of 0.375 Å was used for the local search. For each calculation, 100 docking runs were performed by using a population of 200 individuals and an energy evaluation number of 3 × 10⁶. For the Glide-based analysis, the protein structure was prepared by using the Maestro 8.5 protein preparation wizard (Schrodinger, LLC, 2008, New York, NY); water molecules were deleted, bond orders assigned, and hydrogen atoms added. Next, the orientation of hydroxyl groups, amide groups of Asn and Gln, and the charge state of the His residues were optimized. Finally, a restrained minimization of the protein structure was performed by using the default constraint of 0.30 Å RMSD and the OPLS 2001 force field. The prepared protein structure was used for the subsequent docking calculations. A grid box of default size (20 × 20 × 20 Å³) was centered on the key binding site defined by Tyr73. Default parameters were used and no constraints were included during grid generation. The extra-precision (XP) docking protocol was employed.^[35] Three docking solutions were found by using this protocol with GlideScores between -3.34 and -7.17 kcal mol⁻¹. For comparison purposes, in the AutoDock runs, four docking solutions were found, within a 15 kJ mol⁻¹ energy threshold. Nevertheless, in both AutoDock and Glide protocols, the best solution showed the typical interactions for the terminal GlcNAc moiety in hevein domains.

Molecular modeling: All the details of the calculations are given in the Supporting Information.

Acknowledgements

This work was partially supported by the Programme franco-chinois de Recherches Avancées (PRA B07-06). Y. Yao thanks the French Embassy in China for a Ph.D fellowship. We also thank the EU for financial support (MRTN CT2006-035546 and MICINN; Spain) and for grants CTQ2006-10874-C02-01 and CTQ2009-8536.

- [1] a) G. Felix, M. Regenass, *Plant J.* **1993**, *4*, 307–316; b) R. F. Dalisay, J. A. Kuc, *Physiol. Mol. Plant Pathol.* **1995**, *47*, 315–327; c) T. Yamaguchi, Y. Ito, *Trends Glycosci. Glycotechnol.* **2000**, *12*, 113–120; d) P. G. Patrick, R. M. S. Helmi, P. S. Herman, *Curr. Opin. Struct. Biol.* **2001**, *11*, 608–616; e) L. L. Walling, *Trends Plant Sci.* **2001**, *6*, 445–447; f) N. Ben-Shalom, C. Aki, *Isr. J. Plant Sci.* **2002**, *50*, 199–206; g) Z.-Y. Zhu, Y.-M. Zhang, T. XU, *Acta Phytopathol. Sin.* **2004**, *34*, 231–236.
- [2] a) D. Roby, A. Gabelle, A. Toppan, *Biochem. Biophys. Res. Commun.* **1987**, *143*, 885–892; b) R. B. Day, M. Okada, Y. Ito, *Plant Physiol.* **2001**, *126*, 1162–1173; c) K. Tsukada, M. Ishizaka, Y. Fujisawa, Y. Iwasaki, T. Yamaguchi, E. Minami, N. Shibuya, *Physiol. Plant.* **2002**, *116*, 373–382.
- [3] P. Vander, K. M. Varum, A. Domard, *Plant Physiol.* **1998**, *118*, 1353–1359.
- [4] D. Zhang, M. Hrmova, *Plant Mol. Biol.* **2004**, *54*, 353–372.
- [5] P. P. G. van der Holst, H. R. M. Schlaman, *Curr. Opin. Struct. Biol.* **2001**, *11*, 608–616.
- [6] N. Ben-Shalom, N. Kudabeava, R. Pinto, *Isr. J. Plant Sci.* **2002**, *50*, 259–263.
- [7] Y.-P. Yao, Z.-Y. Zhu, T. Xu, Y.-M. Zhang, *Chem. J. Chinese Universities* **2007**, *28*, 265–269.
- [8] a) J. O. Kihlberg, D. A. Leigh, D. Bundle, *J. Org. Chem.* **1990**, *55*, 2860–2863; b) R. Liang, L. Yan, J. Loebach, *Science* **1996**, *274*, 1520–1522.
- [9] R. K. Jain, K. L. Matta, *Carbohydr. Res.* **1992**, *226*, 91–100.
- [10] *NMR Spectroscopy of Glycoconjugates* (Eds: J. Jiménez-Barbero, T. Peters), Wiley-VCH, Weinheim, **2002**.
- [11] P. Groves, M. Rasmussen, M. D. Molero, E. Samain, F. J. Cañada, H. Driiguez, J. Jiménez-Barbero, *Glycobiology* **2004**, *14*, 451–456.
- [12] D. A. Case, T. E. Cheatham III, T. Darden, H. Gohlke, R. Luo, K. M., Jr. Merz, A. Onufriev, C. Simmerling, B. Wang, R. J. Woods, *J. Comput. Chem.* **2005**, *26*, 1668–.
- [13] N. L. Allinger, Y. H. Yuh, J. H. Lii, *J. Am. Chem. Soc.* **1989**, *111*, 8551–8566.
- [14] Maestro, A powerful, all-purpose molecular-modeling environment, Schrodinger LLC, **2005**.
- [15] H. J. C. Berendsen, J. P. M. Postma, W. F. van Gunsteren, A. Di Nola, J. R. J. Haak, *Chem. Phys.* **1984**, *83–91*, 3684–3690.
- [16] J. L. Asensio, F. J. Canada, A. Garcia-Herrero, M. T. Murillo, A. Fernández-Mayoralas, B. A. Johns, K. Janusz, Z. Zhu, C. R. Johnson, J. Jiménez-Barbero, *J. Am. Chem. Soc.* **1999**, *121*, 11318–11329.
- [17] K. Bock, J. O. Duus, *J. Carbohydr. Chem.* **1994**, *13*, 513–543.
- [18] K. N. Kirschner, R. J. Woods, *Proc. Natl. Acad. Sci. USA* **2001**, *98*, 10541–10545.
- [19] J. L. Asensio, F. J. Canada, H. C. Siebert, J. Laynez, A. Poveda, P. M. Nieto, U. M. Soedjanaamadja, H. J. Gabius, J. Jimenez-Barbero, *Chem. Biol.* **2000**, *7*, 529–543.
- [20] See, for instance: J. F. Espinosa, J. L. Asensio, J. L. Garcia, J. Laynez, M. Bruix, C. Wright, H. C. Siebert, H. J. Gabius, F. J. Canada, J. Jimenez-Barbero, *Eur. J. Biochem.* **2000**, *267*, 3965–3978.
- [21] As a recent example, see, for instance: M. Kolympani, M. Fontanel-la, C. Venturi, S. André, H.-J. Gabius, J. Jiménez-Barbero, P. Vogel, *Chem. Eur. J.* **2009**, *15*, 2861–2873.
- [22] B. Meyer, T. Peters, *Angew. Chem.* **2003**, *115*, 890–918; *Angew. Chem. Int. Ed.* **2003**, *42*, 864–890.
- [23] M. Mayer, B. Meyer, *J. Am. Chem. Soc.* **2001**, *123*, 6108–6117.
- [24] For a typical application of trnOE experiments in the carbohydrate field, see, for instance: J. L. Asensio, J. F. Espinosa, H. Dietrich, F. J. Cañada, R. R. Schmidt, M. Martín-Lomas, S. Andre, H. J. Gabius, J.

- Jiménez-Barbero, *J Am Chem. Soc.* **1999**, *121*, 8995–9000; for further recent examples, see: a) R. S. Houliston, N. Yuki, T. Hiram, N. H. Khieu, J.-R. Brisson, M. Gilbert, H. C. Jarrell, *Biochemistry* **2007**, *46*, 36–44; b) T. Haselhorst, H. Blanchard, M. Frank, M. J. Kraschnefski, M. J. Kiefel, A. J. Szyzew, J. C. Dyason, F. Fleming, G. Holloway, B. S. Coulson, M. von Itzstein, *Glycobiology* **2006**, *17*, 68–81.
- [25] H. C. Siebert, C. W. von der Lieth, R. Kaptein, J. J. Beintema, K. Dijkstra, N. van Nuland, U. M. S. Soedjanaatmadja, A. Rice, J. F. G. Vliegthart, C. S. Wright, H. J. Gabius, *Proteins* **1997**, *28*, 268–284.
- [26] G. M. Morris, D. S. Goodsell, R. S. Halliday, R. Huey, W. E. Hart, R. K. Belew, A. J. Olson, *J. Comput. Chem.* **1998**, *19*, 1639–1647.
- [27] a) R. A. Friesner, J. L. Banks, R. B. Murphy, T. A. Halgren, J. J. Klicic, D. T. Mainz, M. P. Repasky, E. H. Knoll, M. Shelley, J. K. Perry, D. E. Shaw, P. Francis, P. S. Shenkin, *J. Med. Chem.* **2004**, *47*, 1739–1749; b) T. A. Halgren, R. B. Murphy, R. A. Friesner, H. S. Beard, L. L. Frye, W. T. Pollard, J. L. Banks, *J. Med. Chem.* **2004**, *47*, 1750–1759.
- [28] J. Jimenez-Barbero, F. J. Canada, J. L. Asensio, N. Aboitiz, P. Vidal, A. Canales, P. Groves, H. J. Gabius, H. C. Siebert, *Adv. Carbohydr. Chem. Biochem.* **2006**, *60*, 303–354.
- [29] D. A. Case, T. A. Darden, T. E. Cheatham III, C. L. Simmerling, J. Wang, R. E. Duke, R. Luo, K. M. Merz, Jr. D. A. Pearlman, M. Crowley, R. C. Walker, W. Zhang, B. Wang, S. Hayik, A. E. Roitberg, G. Seabra, K. F. Wong, F. Paesani, X. Wu, S. Brozell, V. Tsui, H. Gohlke, L. Yang, C. Tan, J. Mongan, V. Hornak, G. Cui, P. Beroza, D. H. Mathews, C. E. A. F. Schafmeister, W. S. Ross, P. A. Kollman, AMBER 9, University of California, San Francisco, **2006**.
- [30] C. I. Bayly, P. Cieplak, W. D. Cornell, P. A. Kollman, *J. Phys. Chem.* **1993**, *97*, 10269–10280.
- [31] Gaussian 98, M. J. Frisch, G. W. Trucks, H. B. Schlegel, G. E. Scuse-ria, M. A. Robb, J. R. Cheeseman, V. G. Zakrzewski, J. A. Montgomery, Jr., R. E. Stratmann, J. C. Burant, S. Dapprich, J. M. Millam, A. D. Daniels, K. N. Kudin, M. C. Strain, O. Farkas, J. Tomasi, V. Barone, M. Cossi, R. Cammi, B. Mennucci, C. Pomelli, C. Adamo, S. Clifford, J. Ochterski, G. A. Petersson, P. Y. Ayala, Q. Cui, K. Morokuma, D. K. Malick, A. D. Rabuck, K. Raghavachari, J. B. Foresman, J. Cioslowski, J. V. Ortiz, B. B. Stefanov, G. Liu, A. Liashenko, P. Piskorz, I. Komaromi, R. Gomperts, R. L. Martin, D. J. Fox, T. Keith, M. A. Al-Laham, C. Y. Peng, A. Nanayakkara, C. Gonzalez, M. Challacombe, P. M. W. Gill, B. G. Johnson, W. Chen, M. W. Wong, J. L. Andres, M. Head-Gordon, E. S. Replogle, J. A. Pople, Gaussian, Inc., Pittsburgh, PA, **1998**.
- [32] K. N. Kirschner, A. B. Yongye, S. M. Tschampel, J. González-Outeir-ño, C. R. Daniels, B. L. Foley, R. J. Woods, *J. Comput. Chem.* **2008**, *29*, 622–655.
- [33] J. P. Ryckaert, G. Ciccoti, H. J. C. Berendsen, *J. Comput. Phys.* **1977**, *23*, 327–341.
- [34] T. A. Darden, D. York, L. G. Pedersen, *J. Chem. Phys.* **1993**, *98*, 10089–10092.
- [35] R. A. Friesner, R. B. Murphy, M. P. Repasky, L. L. Frye, J. R. Green-wood, T. A. Halgren, P. C. Sanschagrin, D. T. Mainz, *J. Med. Chem.* **2006**, *49*, 6177–6196.

Received: October 16, 2009
Published online: March 12, 2010